Continental Shelf Research 31 (2011) 356–365

Contents lists available at ScienceDirect

Continental Shelf Research

journal homepage: www.elsevier.com/locate/csr

Siliceous productivity changes in Gulf of Ancud sediments (42°S, 72°W), southern Chile, over the last ~150 years

Lorena Rebolledo [a,b,*], Humberto E. González [a,b,c,d], Práxedes Muñoz [e], José L. Iriarte [c,d,f], Carina B. Lange [b,c,d,g], Silvio Pantoja [b,c,d,g], Marco Salamanca [g]

[a] Instituto de Biología Marina, Facultad de Ciencias, Universidad Austral de Chile, Casilla 567, Valdivia, Chile
[b] Centro de Investigación Oceanográfica en el Pacífico Sur-Oriental (COPAS), Universidad de Concepción, Casilla 160-C, Concepción, Chile
[c] Programa COPAS Sur-Austral, Universidad de Concepción, Concepción, Chile
[d] Centro de Investigación en Ecosistemas de la Patagonia (CIEP), Bilbao 449, Coyhaique, Chile
[e] Departamento de Biología Marina, Facultad de Ciencias del Mar y Centro de Estudios en Zonas Áridas (CEAZA), Universidad Católica del Norte, Larrondo 1281, Coquimbo, Chile
[f] Instituto de Acuicultura, Centro de Investigación en Nutrición (CIEN), Universidad Austral de Chile, Casilla 1327, Puerto Montt, Chile
[g] Departamento de Oceanografía, Universidad de Concepción, Casilla 160-C, Concepción, Chile

ARTICLE INFO

Article history:
Received 17 November 2009
Received in revised form
16 June 2010
Accepted 23 June 2010
Available online 21 July 2010

Keywords:
Productivity
Siliceous microfossil
Geochemical proxies
Sediments
Gulf of Ancud
Chile

ABSTRACT

We evaluated changes in siliceous export production and the source of organic matter preserved in sediment core MD07-3109H recovered from the Gulf of Ancud, Chiloé Inner Sea (42°S, 72°W, water column depth: 328 m), southern Chile. We analyzed the abundance of siliceous microfossils (diatoms, silicoflagellates, sponge spicules, Chrysophyte cysts, phytoliths), geochemical proxies (weight percent silicon $\%Si_{OPAL}$, organic carbon, total nitrogen, C/N molar), and sediment stable isotopes ($\delta^{13}C_{org}$, $\delta^{15}N$). Chronology based on ^{210}Pb and ^{14}C provided an accumulated age of 144 years at the base of the core.

Sediments of core MD07-3109H are predominantly marine in origin, averaging $\delta^{13}C_{org} = -20.75‰ \pm 0.82$, $\delta^{15}N = 8.7 \pm 0.35‰$, and $C/N = 8.76 \pm 0.36$. Marine diatoms compose 94% of the total assemblage of siliceous microfossils. Our record of productivity based on the mass accumulation rates of organic carbon, total nitrogen, Si_{OPAL}, and total diatoms showed high values between 1863 and 1869 AD followed by a declining trend until 1921 AD, a transition period from 1921 to 1959 AD with fluctuating values, and a clear decreasing pattern from 1960 AD to the present. This marked reduction in productivity was associated with decreased precipitation and Puelo River streamflow (41°S), as well as a warmer and more stratified water column, especially since the 1980s.

1. Introduction

The Chilean fjord region is an extensive latitudinal area (41–56°S) of channels, fjords, and bays that were formed by glacial erosion during the Quaternary and tectonic sinking of the central Chilean valley (Borgel, 1970). Local remnants of the Last Glacial Maximum ice coverage include the North Patagonian Icefield (46–47°S), South Patagonian Icefield (48–52°S), and the Darwin Mountains Icefield in Tierra del Fuego (54–55°S), covering a total area of 19,000 km^2 (Warren and Aniya, 1999).

The Chilean fjord region is important for paleoclimate studies since it is highly sensitive to variations in the Southern Westerlies, which are responsible for high precipitation (~2000–7000 mm yr^{-1}; Miller, 1976) and maximum river discharges at 42°, 46°, and 50°S (Dávila et al., 2002). Moreover, the high sedimentation rates in this area allow for high temporal resolution paleoclimate studies.

Several authors have studied the geochemistry of recent sediments in Chilean fjords (e.g., Silva and Prego, 2002; Salamanca and Jara, 2003; Ahumada and Rudolph, 2004; Pinto and Bonert, 2005; Rojas and Silva, 2005; Sepúlveda et al., 2005, this issue; Mulsow et al., 2009; Silva et al., this issue). Recently, Silva et al. (2009) showed evidence of changes in the sources of the organic matter (C/N, $\delta^{13}C$) in surface sediments from the Inner Sea of Chiloé associated with greater contributions of terrigenous matter in areas near rivers. In addition, it is important to note that the area of the northern fjords (41–44°S) is characterized by commercial aquaculture and industrial activities (Otero, 2006; Buschmann et al., 2009).

Few sediment studies have focused on the temporal variability (downcore) in assemblages of siliceous microfossils preserved in the sediments and the fluctuations in sources of organic matter. At present, the studies that have been carried out in the Puyuhuapi Channel near the Northern Patagonian Icefield

* Corresponding author at: Instituto de Biología Marina, Facultad de Ciencias, Universidad Austral de Chile, Casilla 567, Valdivia, Chile. Tel.: +56 41 220 3557; fax: +56 41 220 7254.
E-mail address: lrebolle@udec.cl (L. Rebolledo).

0278-4343/$ - see front matter © 2010 Elsevier Ltd. All rights reserved.
doi:10.1016/j.csr.2010.06.015

revealed dramatic changes in the siliceous productivity of the last century associated with changes in rainfall, terrigenous contributions, and El Niño events (Rebolledo et al., 2005; Sepúlveda et al., 2005). On a larger temporal scale, paleoceanographic studies carried out in the area of the Jacaf Fjord, Northern Patagonia, have also shown fluctuations in siliceous productivity, sea surface temperature (SST), and precipitation based on geochemical proxies over the past 2000 years (Rebolledo et al., 2008; Sepúlveda et al., 2009) associated with the Little Ice Age (LIA) and the Medieval Warm Period (MWP), both widely reported in the Northern Hemisphere and less frequently studied in the Southern Hemisphere. Furthermore, fluctuations in the San Rafael glacier have also been related to these contrasting climatic periods (Araneda et al., 2007).

The objective of this research was to study the variability in siliceous export production preserved in the sediments of the Gulf of Ancud (42°S) over the last century. Based on the content of siliceous microfossils (diatoms, silicoflagellates, phytoliths, Chrysophyte cysts) and geochemical proxies (%Si_{OPAL}, organic carbon C_{org}, nitrogen N_{tot}, C/N molar, sediment stable isotopes $\delta^{13}C_{org}$ and $\delta^{15}N$), our record offers evidence of changing productivity related to Pacific-wide (e.g., El Niño) and local-scale events (e.g., rainfall, Puelo River streamflow).

2. Study area

The Inner Sea of Chiloé (41–43°S; Fig. 1) is connected to the open ocean on the north through the Chacao Channel and on the south through the Boca del Guafo Passage. This area consists of four micro-basins (Reloncaví Fjord, Reloncaví Sound, Gulf of Ancud, Gulf of Corcovado) interconnected through narrow passes between islands that give rise to bathymetric constrictions and sills; these contribute to reducing the water flow between micro-basins (Silva et al., 2009), probably leading to long residence time of the waters. One of the most important of these constriction sills is the Desertores Pass, which is 5 km wide, 20 m long, and has a maximum depth of 200 m. Two main water masses are found in this area: Subantarctic Water and Modified Subantarctic Water (influenced by freshwater influxes from rivers). The bathymetric constriction in the Gulf of Corcovado (Desertores Pass) impedes the penetration of Equatorial Subsurface Waters to the north of the pass (Silva et al., 1995). The tide in the Chiloé Inner Sea is largely semi-diurnal with variations of up to 6 m (Cáceres et al., 2003).

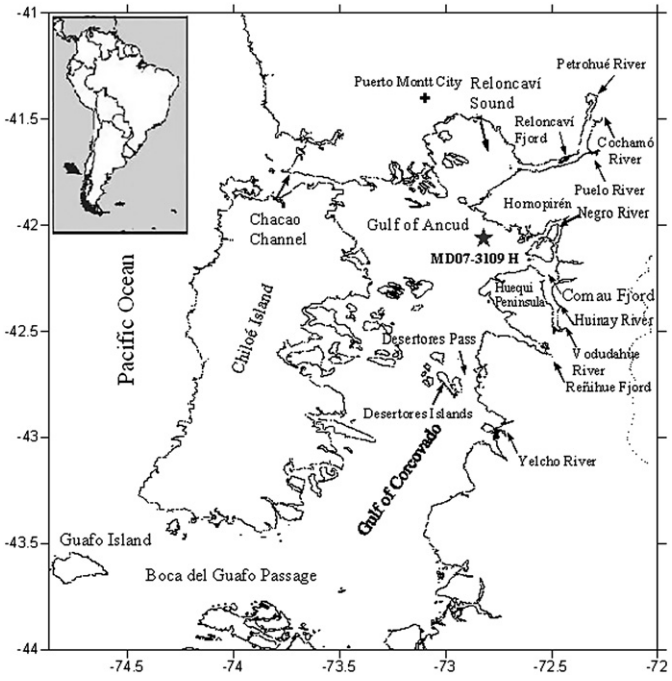

Fig. 1. Map of the study area showing the Inner Sea of Chiloé, the main rivers in the area, and names of gulfs and passages referred to in the text. The star indicates the sampling site of core MD07-3109H.

In the Inner Sea of Chiloé and along the coasts of the fjords, primary productivity is high, with mean values between 0.5 and 3 g C m^{-2} d^{-1} (Iriarte et al., 2007), and chlorophyll-*a* reaches 0.1–12 mg m^{-3} (Iriarte et al., 2007; Tello and Rodríguez-Benito, 2009). Phytoplankton studies of the water column between Puerto Montt and Laguna San Rafael (41–46°S) show a predominance of *r*-strategist diatoms and small species of the genus *Thalassiosira* and *Skeletonema costatum*. The greatest phytoplankton cell concentrations are distributed between the Reloncaví Sound and the Gulf of Corcovado, at the head of Moraleda Channel, and in the Puyuhuapi Channel (Avaria et al., 1997).

Dissolved inorganic nutrients (orthophosphate and nitrate) in the Inner Sea of Chiloé are contributed mainly by the oceanic waters, whereas silicic acid is provided by the rivers (Silva et al., 1997). In winter and spring, the study area is characterized by sea surface temperatures of 10–14 °C, salinity ranging from 29 to 33 psu, and inorganic nutrient concentrations of nitrate between 0.5 and 20 μM, silicic acid between 4 and 30 μM, and orthophosphate between 0.5 and 3.0 μM (CENDHOC, 2009; González et al., 2010).

The rivers in this area have a pluvio-nival regime, with the greatest discharges in the rivers Puelo (678 m^3 s^{-1}), Yelcho (363 m^3 s^{-1}), and Petrohué (278 m^3 s^{-1}), followed by the rivers Reñihue (60 m^3 s^{-1}) and Cochamó (20 m^3 s^{-1}) (Dirección General de Aguas, DGA, 2005). The Comau Fjord (Fig. 1), which is 46 km long, 1–3 km wide, and has an average depth of 250 m and a maximum depth of 450 m. Three important rivers (Vodudahue, Huinay, Negro) discharge directly into this fjord. Discharges are usually higher in autumn–winter (April–August) and spring (November–December) and lower in summer to early autumn (January–March). Urrutia et al. (2005) reported a direct relationship between precipitation and freshwater discharge, especially in the winter months.

3. Material and methods

3.1. Core collection

The core analyzed in this study (MD07-3109H) was obtained during the PACHIDERME cruise in February 2007 on board the R/V *Marion Dufresne* (MD 159). The sediment core was collected at the mouth of the Comau Fjord (42°03′S, 72°49′W; water column depth: 328 m; core length: 28 cm) in the Gulf of Ancud (Fig. 1). We used a "HAP_S corer", which is an automatic metal instrument with an acrylic tube (11 cm in diameter) that allows cores to be obtained intact, without altering the water–sediment interface (OceanTest Equipment Inc., 2010).

The core was sliced at 0.5-cm intervals in the first 10 cm and at 1-cm intervals from there until the bottom (28 cm). The samples were labeled and stored in plastic bags and frozen at −20 °C until later analysis in the laboratory. The bulk grain size was analyzed with the same resolution previously described using a Mastersizer 2000 laser diffraction particle size analyzer. Wet sediment samples were introduced into a deionized water tank free of additive dispersant split with a 2000 rpm stirrer and sonicated during 180 s. The sample quantity was adjusted in order to obtain a laser beam obscuration between 10% and 20%.

The water content in the sediment layers was calculated based on the difference between wet weight and dry weight. Dry bulk density was calculated according to the equation: density ($g\,cm^{-3}$)=dry mass/[(dry mass/2.65 $g\,cm^{-3}$)+(water mass/1.025 $g\,cm^{-3}$)], where 2.65 is the density of the solids and 1.025 is the water density (Bloesch and Evans, 1982).

3.2. Dating

The geochronology was established using the ^{210}Pb dating method by alpha spectrometry of its daughter ^{210}Po (secular equilibrium). This was done with ~0.5 g dry sediment, adding ^{209}Po as a tracer and a mixture of concentrated acids (HCl, HNO_3, and HF). The solutions were deposited on silver plates at 75 °C and left in the presence of ascorbic acid for 2.5 h (Flynn, 1968). The activities were counted in a CANBERRA QUAD alpha spectrometer, model 7404, during 24–48 h to achieve the desired counting statistics (4–10% 1σ errors). The excess activities (unsupported) were estimated from the total minus the supported (background) activities established from the exponential decay of ^{210}Pb. The supported value obtained was assumed to be in equilibrium with ^{226}Ra (McCaffrey and Thomson, 1980; Cochran et al., 1998). The unsupported (^{210}Pb) or "in excess" ($^{210}Pb_{xs}$) inventories, expressed in dpm cm^{-2}, were calculated according to Turekian et al. (1980), where $I=\Sigma A_i\rho_i h_i$, A_i is $^{210}Pb_{xs}$ (dpm g^{-1}), ρ_i is the dry bulk density for interval i ($g\,cm^{-3}$), and h is the thickness of the interval in cm. The activities were corrected for the decay of ^{210}Po (half-life: 138 days) between plating and counting. The standard deviations of the inventories and ages were estimated from the propagation of counting uncertainties and the error of the supported estimation of ^{210}Pb (Bevington and Robinson, 1992).

The chronology of core MD07-3109H was determined using the Constant Rate of Supply model (Appleby and Oldfield, 1978; Turekian et al., 1980; Cochran et al., 1998), which assumes a constant flow of $^{210}Pb_{xs}$ to the sediment, allowing us to determine the recent sedimentation rate and the age of the layers in the respective intervals.

In addition, bulk sediment ^{14}C was determined for one sample (26–27 cm) at the National Ocean Sciences Mass Spectrometry Facility (NOSAMS). We weighed ~100 mg of freeze-dried sediment. The sample was then subjected to acid pre-treatment with H_3PO_4 to remove inorganic carbon and subsequently combusted at high temperature to produce CO_2, which was transferred to a reaction tube for reduction to pure carbon (graphite) and then placed into target cartridges for loading into the accelerator mass spectrometer (AMS). Measurement precision was 5–7%. ^{14}C ages were calibrated to AD years using the CALIB 5.0.2 (2009) software, which provided a 95% confidence interval (Table 1).

3.3. Geochemical analyses

Analyses of C_{org}, N_{tot}, and carbon and nitrogen stable isotopes (δ^{15}N, $\delta^{13}C_{org}$) were conducted at the University of California Davis Stable Isotope Facility, USA. Sediments samples were freeze-dried, ground, placed in aluminum cups, and then exposed to acid vapors (HCl 12 N) in a dessicator for 4 h in order to remove the inorganic carbon. About 40 mg of the acid-treated sample were transferred to tin cups. A PDZ Europa ANCA-GSL elemental analyzer was used to measure C_{org} and N_{tot} (analytical precision ±0.16% for nitrogen and ±0.02% for carbon), and a PDZ Europa 20–20 continuous flow isotope ratio mass spectrometer was used for the stable isotopes of N and C. Values are expressed in delta notation: for nitrogen: $\delta^{15}N\ (‰)=[(^{15}N/^{14}N)_{sample}/(^{15}N/^{14}N)_{standard}-1]\times 1000$ with N_2 in air as a reference; for carbon: $\delta^{13}C_{org}\ (‰)=[(^{13}C/^{12}C)_{sample}/(^{13}C/^{12}C)_{standard}-1]\times 1000$ with Pee Dee Belemnite as a reference. The analytical precision was ±0.19‰ for δ^{15}N and ±0.10‰ for $\delta^{13}C_{org}$.

We determined the weight percent silicon using the method proposed by Mortlock and Froelich (1989). Data are expressed as: content of Si_{OPAL} ($mg\,g^{-1}$)=$112.4\times(C_s/M)\times 10$, where C_s is the silica concentration in the sample in mM, M the sample mass in milligrams, and 112.4 the molecular weight of Si (28.09) × the extraction volume of NaOH (0.04 L) × 100.

The geochemical proxies (Si_{OPAL}, C_{org}, N_{tot}) are expressed in $mg\,g^{-1}$ of dry sediment. Mass accumulation rates (MAR_S) were calculated as: concentration × dry bulk density × sedimentation rate.

The chlorinity content was not determined for our samples, and thus, the geochemistry data were not corrected for salt content.

3.4. Microfossil counts

For siliceous microfossils (diatoms, silicoflagellates, sponge spicules, Chrysophyte cysts, phytoliths), wet sediment samples were freeze-dried and ~0.5 g of dry sediment was treated according to the technique described in Schrader and Gersonde (1978). Permanent slides were prepared by placing a defined sample volume (0.2 mL) onto a microscope slide that was then air-dried and mounted with Naphrax mounting medium (refraction index=1.7). Two permanent slides per sample were prepared in this fashion.

Diatom and silicoflagellate species were identified and counted under a Zeiss Axioskop 2 plus microscope. A fraction (1/10) of the slide area was chosen and two slides per sample were counted; the estimated counting error was 15%. Because of the high abundance of Chaetoceros resting spores, these were counted along defined transects at 1000 ×. Total diatom abundances are given in valves g^{-1} of dry sediment.

Diatoms were identified to the lowest taxonomic level possible, based principally on the works of Cupp (1943), Rivera (1981), Round et al. (1990), Sims (1996), Witkowski et al. (2000), and Rebolledo et al. (2005). In order to summarize the fluctuations of the diatoms, these were grouped by ecological affinity into the following categories: high nutrient (HN), coastal planktonic (CP), non-planktonic (NP), freshwater (FW), warm water (WW), and cold water (CW) (Table 2).

Moreover, we calculated diatom diversity as the Shannon–Wiener diversity index: $H'=-\Sigma pi\log pi$, where $pi=n_i/N$ or the proportion of the total number of individuals per species in each sample, n_i the number of individuals per species, and N the total number of individuals per sample (Brower et al., 1998).

Table 1
Radiocarbon dates and their calibrated ages for core MD07-3109H determined using the software Calib 5.0.2. (2009). The ΔR was estimated for the difference between the age calculated with the ^{210}Pb model and the corresponding ^{14}C age.

Laboratory number	Core depth (cm)	Material	^{14}C-AMS age (yr BP)	Error (yr)	ΔR (1σ)	Calibrated age cal yr AD (1σ)
OS-73721	26–27	Bulk sediment	970	30	488 ± 38	1880 ± 100

Table 2
Diatom ecological groups defined on the basis of their habitat, according to Cupp (1943), Round et al. (1990), Sims (1996), Witkowski et al. (2000), and Rebolledo et al. (2005).

High nutrients (HN)
Resting spores *Chaetoceros* spp.
Chaetoceros cinctus Gran
Ch. constrictus Gran
Ch. coronatus Gran
Ch. debilis Cleve
Ch. diadema (Ehrenberg) Gran
Ch. didymus Ehrenberg
Ch. radicans Shütt
Ch. vanheurckii Gran
Skeletonema costatum (Greville) Cleve
Thalassionema nitzschioides var.
nitzschioides (Grunow) Grunow
Cold water (CW)
Thalassiosira gerloffii Rivera
T. pacifica Gran and Angst
Stellarima microtrias (Ehrenberg) Hasle & sims
Rhizosolenia borealis Sundström
Warm water (WW)
Coscinodiscus janischii Schmidt
Thalassiosira ferelineata Hasle and Fryxell
Odontella longicruris (Greville) Hoban
Chaetoceros lorenzianus Grunow
Thalassiosira mendiolana Hasle and Heimdal
Thalassionema nitzschioides var. *inflata* Koebe
Thalassionema nitzschioides var. *parva* (Heiden) Moreno-Ruiz
Non-Planktonic (NP)
Actinoptychus senarius Ehrenberg (Ehrenberg)
A. vulgaris Schumann
Auliscus sp.
C. californica var. *antarctica* Grunow
C. californica var. *californica* Grunow
C. costata var. *costata* Gregory
C.costata var. *pacifica* Grunow
C. scutellum var. *parva*
C. scutellum var. *scutellum* (Ehrenberg)
Cocconeis spp.
Dimmeregrama minor (Gregory) Ralfs in Pritchard
Diploneis didyma (Ehrenberg) P.T Cleve
D. interrupta (Kützing) Cleve
D. *splendida* var. *puella (*A. Schmidt in Schmidt et al.) Cleve
Diploneis spp.
Grammatophora angulosa Ehrenberg
G. marina (Lyngbye) Kützing
Hyalodiscus scoticus (Kützing) Grunow
H. stelliger Bailey
Melosira arctica Dickie
M. nummuloides (Dillwyn) C.A Agarh
M. lineata (Dillwyn) Agardh
Opephora pacifica (Grunow) Petit
Paralia sulcata (Ehrenberg) Cleve
Plagiogramma interruptum (Gregory) Ralfs
Podosira sp.
Psammodictyon panduriforme (Gregory) Mann
Pseudohimantidium pacificum Hustedt and Krasske
Rhabdonema sp.
Stictodiscus californicus R.K. Greville
Surirella spp.

Coastal planktonic (CP)
Actinocyclus curvatulus Janisch
A. octonarius var. *sparsa* (Greg.) Hustedt
Actinocyclus sp.
Asteromphalus heptactis (Brébisson) Ralfs
Bacteriastrum sp.
Coscinodiscus radiatus Ehrenberg
C. marginatus Ehrenberg
C. perforatus Ehrenberg
Cyclotella litoralis Lange and Syvertsen
Ditylum brightwellii (West) Grunow
Lauderia annulata Cleve
Pseudo-nitzschia pungens (Grunow and Cleve) Hasle
Rhizosolenia setigera Brigthwell
R. pungens Cleve
Rhizosolenia sp.
Sthephanophyxis turris (Greville and Arnott) Ralfs
Thalassiosira aestivalis Gran and Angst
T. angulata (A. Schmidt) Hasle
T. anguste-lineata (A. Schmidt) G. Fryxell and Hasle
T. decipiens (Grunow) Jørgensen
T. delicatula (*chilensis*) Ostenfeld (in Bogert)
T. eccentrica (Ehrenberg) Cleve
T. oestrupii var. *venrickae* G. Fryxell and Hasle
T. tenera Proschkina-Lavrenko
T. sp.
T. spp. (5–12 μm)
Freshwater (FW)
Achnantes spp.
Amphora sp.
Aulacoseira granulata (Ehrenberg) Ehrenberg
Bacillaria paxillifer (O.F Müller) Hendey
Chaetoceros muelleri Lemmerman
Cyclotella ocellata Pantocsek
C. meneghiniana Kützing
C. stelligera (Cleve and Grunow) Van Heurck
Cyclotella spp.
Diatoma spp.
Epithemia zebra (Ehrenberg) Kützing
Eunotia sp.
Eunotograma laevis Grunow
Fragilaria construens var. *venter* (Ehrenberg) Grunow
Fragilaria sp.
Frustrulia sp.
Gomphonema constrictum Ehrenberg
Hantzschia amphioxys (Ehrenberg) Grunow
Hannaea arcus (Ehrenberg) Patrick
Melosira spp.
Navicula decussis Oestrup
Navicula forcipata Greville
Navicula palpebralis Brébisson and Smith
Navicula sp.
Nitzschia frustrulum H. Bennion
Nitzschia sp.
Pinnularia sp.
Rhoicosphenia curvata (*Kützing*) *Grunow*
Rhopalodia gibba (Ehrenberg) Müller
Rhopalodia sp.
Ehrenberg
Synedra sp.
Stephanodiscus astraea (Ehrenberg) Grunow
Tabularia tabulata (Kützing) (C.A Agardh)
Snoeij
Trachyneis aspera (Ehrenberg) Cleve

3.5. Climatic time-series

With the objective of comparing our MARs with climatic series, we used historical rainfall series for the Puerto Montt area (1910–2007, Royal Netherland Meteorological Institute; KNMI, 2009), the Puelo River streamflow (1944–2005; DGA, 2005), reconstructed sea surface temperature (SST) records from 44°S, 76°W grid 2 × 2 (1960–2005; NOAA, 2005), and the Multivariate ENSO Index (MEI) (1950–2007; NOAA, 2009). Data are expressed as anomalies from each series, where we subtracted the average divided by the historic standard deviation of the respective series.

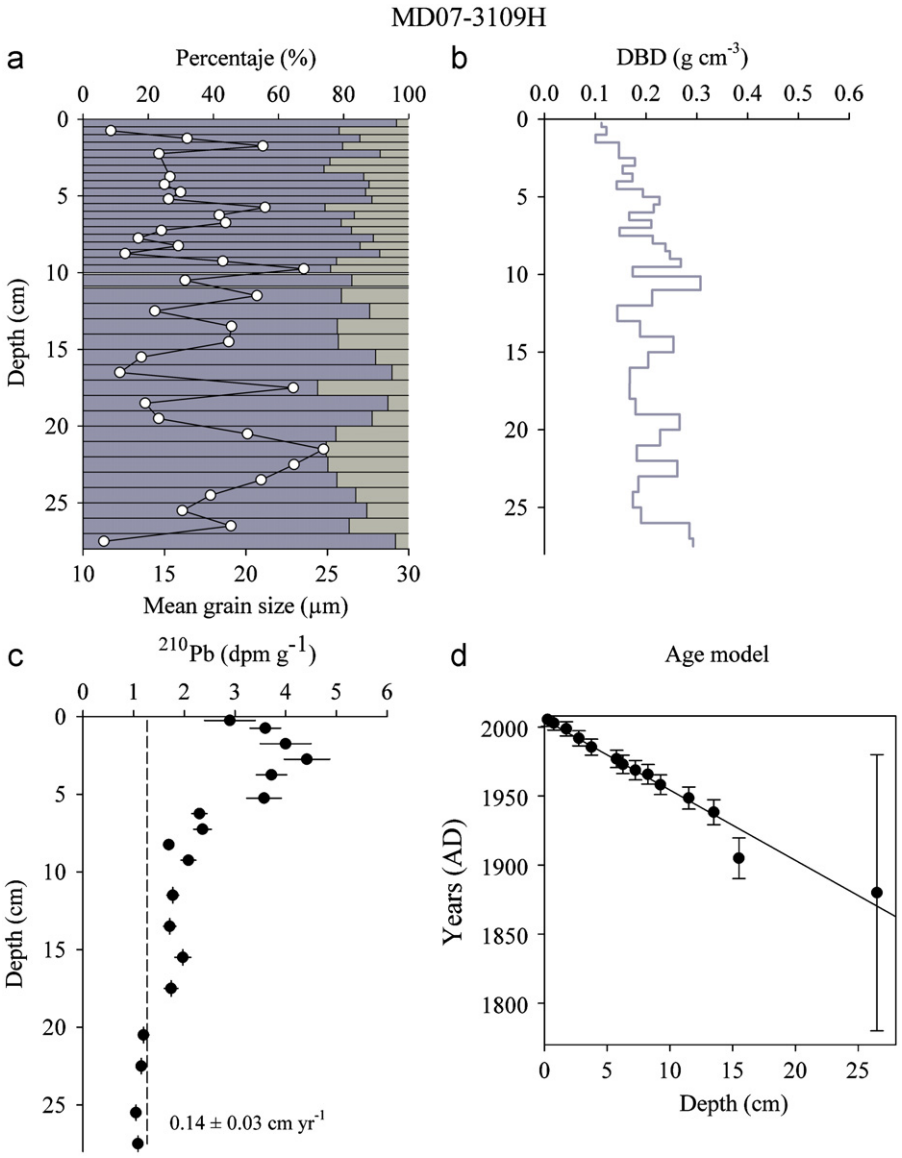

Fig. 2. (a) Silty-clay (<63 μm) and sand (>63 μm) fractions of sediments from the core MD07-3109H; gray and dark bars indicate the percentages of silty-clay and sand, respectively, and white circles represent the mean grain size distribution. (b) Dry bulk density (g cm^{-3}). (c) Vertical distribution of ^{210}Pb (dpm g^{-1}) activity; the horizontal error bars represent one standard deviation (1σ) based on the propagation of ^{210}Pb and the standard deviation of the background. The vertical dotted line is the supported activity (background). (d) Age model for core MD07-3109H based on ^{210}Pb and one ^{14}C datapoint (years AD) *versus* depth in cm. The last bar represents the ^{14}C calibrated age and one standard deviation (1σ) (Table 1).

4. Results

4.1. Sediment characteristics and dating

The sediments of core MD07-3109H were dark and olive black in color (5Y 4/3 and 5Y 3/2 Munsell scale). Mean grain size varied between 11 and 25 μm along the core. The sediments were composed predominantly by silty-clay (83%) with a lower percentage of sand (17%) (Fig. 2a). Dry bulk density values (DBD) oscillated between 0.10 and 0.30 g cm^{-3}, averaging 0.19 ± 0.05 g cm^{-3} and increasing towards the deeper part of the core (Fig. 2b).

The ^{210}Pb activity in the MD07-3109H core fluctuated between 1.2 and 4.5 dpm g^{-1}. Surface values were lower due to a bioturbated layer in the upper 3.5 cm. The activities of the core showed a good exponential fit ($r^2=0.99$, $p<0.01$), allowing estimates of a supported value (background) of 1.27 ± 0.16 dpm g^{-1} at 20.5 cm (Fig. 2c). The $^{210}Pb_{xs}$ (unsupported) below the mixed layer (3.5 cm) revealed a recent sedimentation rate of 0.14 ± 0.03 cm yr^{-1}.

The local water reservoir effect (ΔR) for the area of the Inner Sea of Chiloé was determined from the difference between the global reservoir estimated from the Marine curve 04 (Hughen et al., 2004) for the layer 26–27 cm determined with ^{210}Pb, and the difference with the ^{14}C age estimated at the same stratigraphic level; this resulted in a local reservoir effect of $\Delta R=488 \pm 38$ years (Table 1). The ^{14}C age interval 26–27 cm was recalibrated using this local reservoir. The extrapolation of the ages obtained from the surface to the base of the core allowed us to obtain an accumulated age of 144 years (Fig. 2d).

4.2. Geochemical data and organic matter sources

The C_{org} content ranged between 12.7 (1905 AD) and 32.3 mg g^{-1} (2006 AD), and increased toward the core top (Fig. 3a).

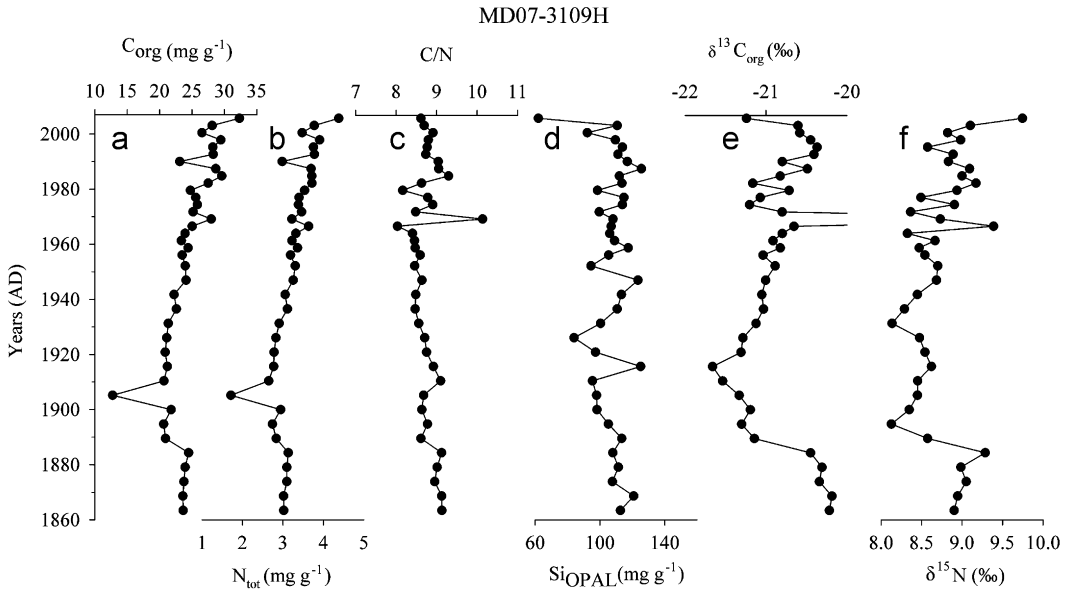

Fig. 3. Geochemical characteristics of the sediments in core MD07-3109H: Contents of (a) organic carbon (C_{org}, mg g^{-1}), (b) nitrogen (N_{tot}, mg g^{-1}), (c) C/N molar, (d) silicon content (Si_{OPAL}, mg g^{-1}), (e) $\delta^{13}C_{org}$ (‰), and (f) $\delta^{15}N$ (‰). The data outside the scale in figure (e) represent a value of $\delta^{13}C_{org} = -16$‰.

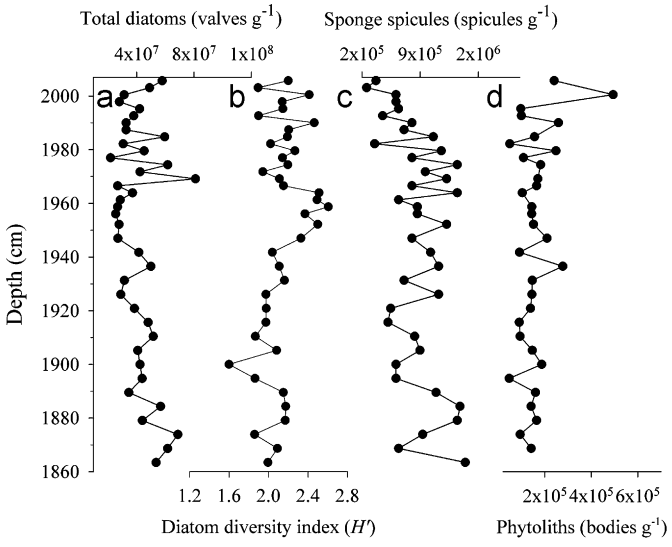

Fig. 4. Concentration of siliceous microfossils in core MD07-3109H: (a) Total diatoms (valves g^{-1}), (b) Shannon diversity index (diatoms), (c) sponge spicules (spicules g^{-1}), and (d) phytoliths (bodies g^{-1}).

The behavior of N_{tot} was similar to that of C_{org}, with values that fluctuated between 1.77 (1905 AD) and 4.44 mg g^{-1} (2006 AD) (Fig. 3b). The C/N molar varied between 8.0 and 10.1; the maximum value of 10.1 corresponded to the 1969 AD interval (Fig. 3c). Overall, a slightly decreasing trend was observed from the base of the core to its surface.

Along the core, the content of Si_{OPAL} decreased from the base of the core to ~1910 AD and from the 1980s to the present (Fig. 3d). Minimum and maximum values were 62 (2006 AD) and 125.6 mg g^{-1} (1987 AD), respectively. Carbon and nitrogen stable isotope records showed fluctuations along the core, with $\delta^{13}C_{org}$ varying between −21.6 (1916 AD) and −16.3‰ (1969 AD), and $\delta^{15}N$ between 8.1 (1895 AD) and 9.7‰ (2006 AD) (Fig. 3e, f).

We calculated the contribution of marine and terrigenous organic matter sources in our core using a mixing equation (e.g., Thornton and McManus, 1994; Sepúlveda et al., this issue and references therein) where % terrigenous = $[(\delta^{13}C_{org\ S} - \delta^{13}C_{org\ M})/(\delta^{13}C_{org\ T} - \delta^{13}C_{org\ M})] \times 100$; % marine = 100 − % terrigenous. $\delta^{13}C_{org}$ S = $\delta^{13}C_{org}$ of a given sample, $\delta^{13}C_{org}$ M = $\delta^{13}C_{org}$ of the marine end-member, $\delta^{13}C_{org}$ T = $\delta^{13}C_{org}$ of the terrigenous end-member. Mixing was estimated using the $\delta^{13}C_{org}$ data for marine ($\delta^{13}C_{org} = -20.2$) and terrigenous ($\delta^{13}C_{org} = -26.3$) end-members for the Chiloé Inner Sea given by Silva et al. (2009). The calculation of the mixing model revealed a predominantly marine contribution of "87%" in our core.

4.3. Abundance of siliceous microfossils and variability in ecological diatom groups

Diatoms were the dominant group (98% of the total assemblage), with an average concentration of 4×10^7 valves g^{-1} (Fig. 4a). Second in importance were sponge spicules, with an average of 8×10^5 spicules g^{-1}, and phytoliths averaged 1.6×10^5 bodies g^{-1} (Fig. 4c, d). Diatom diversity (H') fluctuated between 1.6 (1900 AD) and 2.6 (1960 AD; Fig. 4b). In general, minimum H' values were associated with high abundances of *Chaetoceros* resting spores. In our record, silicoflagellates (with *Distephanus speculum* as the main species) and Chrysophyte cysts presented erratic fluctuations and very low abundances; thus, their data are not shown.

The variability in the six diatom groups (Table 2) showed that the high nutrient (HN) group dominated the diatom assemblage (average 68%) and was mainly represented by resting spores (RS) of the genus *Chaetoceros* (*Chaetoceros radicans/cinctus*, *C. constrictus/vanheurckii*, *C. coronatus*, *C. diadema*). The abundances of *Chaetoceros* RS were always high all along the core (Fig. 5a). The relative abundance of *Thalassionema nitzschioides var. nitzschioides*, which also belongs to the HN group, averaged ~5%. The coastal planktonic (CP) group was mainly represented by *Rhizosolenia pungens*, *Thalassiosira eccentrica*, *Cyclotella litoralis*, *Thalassiosira angulata*, *T. oestrupii var. venrickae*, *Thalassiosira* sp., and *Ditylum brightwelli*. This was the second most important group, with an average contribution of 14% and higher values towards the upper part of the core (Fig. 5b). Within this group, it is interesting to note that *R. pungens* did not occur in sediments older than 1900 AD, and that the abundance of this species increased in the last 20 years.

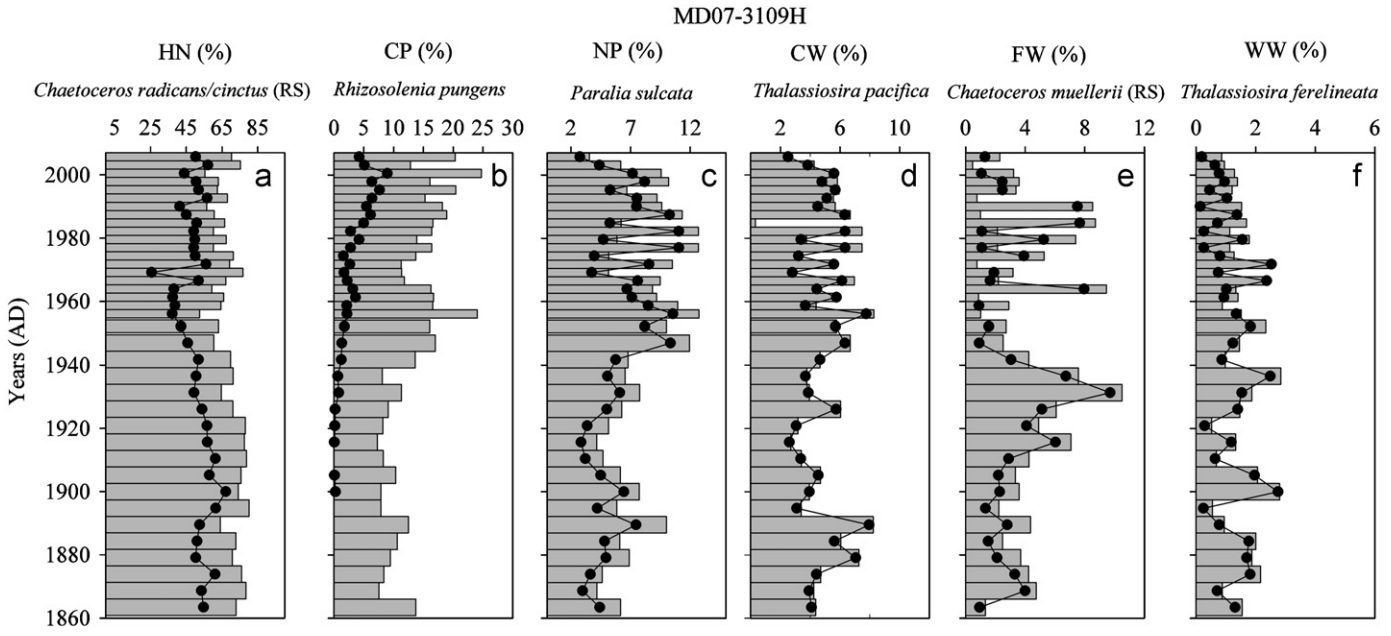

Fig. 5. Principal diatom groups in the sediment record of core MD07-3109H: (a) high nutrient (HN), (b) coastal planktonic (CP), (c) non-planktonic (NP), (d) cold water (CW), (e) freshwater (FW), and warm water (WW). The bars indicate abundance as percentages of the main groups and the black lines show the main representative species of these groups. Please refer to Table 2 for genera and species within diatom groups.

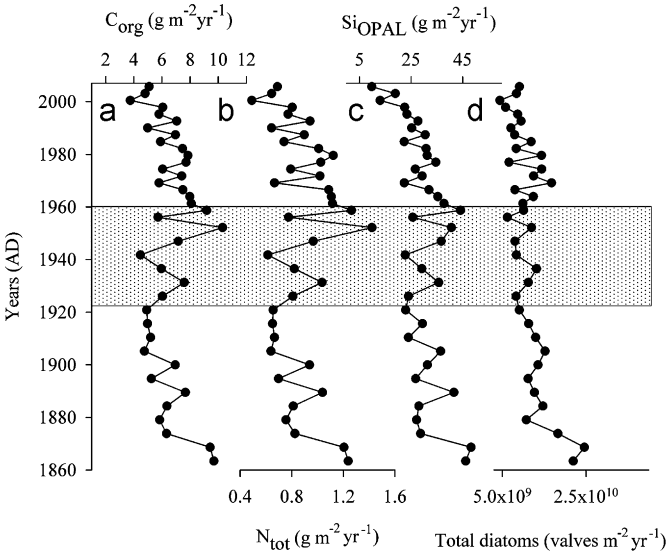

Fig. 6. Mass accumulation rates in core MD07-3109H: (a) C_{org} ($g\,m^{-2}\,yr^{-1}$), (b) N_{tot} ($g\,m^{-2}\,yr^{-1}$), (c) Si_{OPAL} ($g\,m^{-2}\,yr^{-1}$), (d) total diatoms (valves $m^{-2}\,yr^{-1}$). The shaded area represents the transition period mentioned in the text.

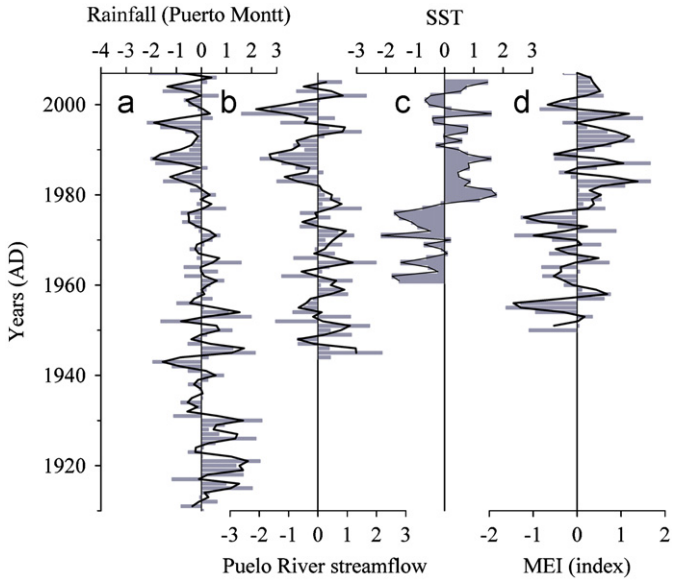

Fig. 7. Anomalies in (a) rainfall for Puerto Montt (1910–2007), (b) the Puelo River streamflow (1944–2005), (c) reconstructed SST (1960–2005) at 44°S, 76°W, 2 × 2 grid, and (d) MEI index (1950–2007). The lines represent a 2-year running mean for all variables.

The non-planktonic (NP) group, whose main components were *Paralia sulcata*, *Actinoptychus senarius*, *Grammatophora marina*, *Cocconeis californica var. californica*, and *Psammodictyon panduriforme*, presented high variability with incremental pulses in 1947, 1957, 1972, 1977, and 1982 AD, followed by a decreasing pattern since ~1988 AD (Fig. 5c). *Paralia sulcata* was the main contributor to this group, with an average abundance of ~6%. The fourth group in importance was the cold water (CW) group, which made an average contribution of 5% and was characterized by *Thalassiosira pacifica*. This group presented higher abundances at the base of the core and a decreasing trend from 1990 AD to the present (Fig. 5d).

The freshwater (FW) group registered an average contribution of 4%. It was composed of many species and genera, with the main contributors *Chaetoceros muellerii* RS, *Cyclotella* sp., *Cyclotella stelligera*, *Cyclotella meneghiniana*, *Synedra* sp., *Rhoicophenia curvata*, *Aulacoseira granulata*, and *Eunotia* sp. This group showed large fluctuations with important pulses of increments in the early 1900s, 1932, 1964, and from the late 1970s through the late 1980s, and a clear decreasing trend to the present (Fig. 5e). *Chaetoceros muellerri* (RS) was the main species in this group. Finally, the contribution of the warm-water group was minor (values $<2\%$ on average), with the lowest abundances occurring

after 1980 AD (Fig. 5f); the dominant taxon was *Thalassiosira ferelineta*.

4.4. Mass accumulation rates (MAR_s)

Average $MARC_{org}$ was 6.57 ± 1.54 g m^{-2} yr^{-1}, with higher values (~ 10 g m^{-2} yr^{-1}) at the base of the core between 1869 and 1863 AD, followed by a decreasing trend until 1921 (< 8 g m yr^{-1}), a transition period (1921–1959 AD) with somewhat higher values (~ 8 g m^{-2} yr^{-1}), and another decreasing trend until 2000 (Fig. 6a). $MARN_{tot}$ averaged 0.87 ± 0.21 g m^{-2} yr^{-1} and had a very similar pattern to that described for $MARC_{org}$ (Fig. 6b).

$MARSi_{OPAL}$ averaged 29.56 ± 8.33 g m^{-2} yr^{-1} with the highest values recorded at the base of the core, followed by lower values until 1921 AD, highly variable values between 1921 and 1959 AD, and a decreasing trend since 1960 (Fig. 6c). MAR of total diatoms varied between 4×10^9 and 2×10^{10} valves m^{-2} yr^{-1} and was highest in the older part of the record. The regression anaysis between $MARSi_{OPAL}$ and the logarithm of MAR total diatoms was significant ($R^2 = 0.26$, $n = 38$, $p < 0.001$).

In general, our MAR records defined two distinct periods (1863–1921 AD and 1960–2006 AD) characterized by a decreasing trend in siliceous productivity and separated by a transition interval of greatly fluctuating values (Fig. 6).

4.5. Climatic time-series

We set the climate scenario of the past 100 years by comparing the standardized anomalies of rainfall for the Puerto Montt area, the Puelo River streamflow, the reconstructed SST for the 44°S, 76°W grid 2×2, and the Multivariate El Niño Index (MEI) (Fig. 7). The standardized precipitation record allowed us to distinguish three periods: (a) 1910–1930 AD, with positive anomalies; (b) 1932–1980 AD, a fluctuating period with many positive and negative anomalies; and (c) 1980–2007 AD, with mainly negative anomalies coinciding with the decline in the Puelo River streamflow since the 1980s (Fig. 7a, b). The reconstructed SST series (1960–2005 AD) for the 44°S, 76°W grid 2×2 area revealed negative anomalies prior to $\sim$1976 AD and mainly positive values from 1980 AD to the present (Fig. 7c). According to the MEI, the interannual and interdecadal variability that occurred from 1950 to 1976 AD was characterized as a cold period, which was followed by a warm interval between 1977 and 1998 AD (Fig. 7d).

5. Discussion

5.1. Sediment characteristics and comparisons with other fjord systems

According to our chronology, the surface sedimentation rate of core MD07-3109H was 0.14 cm yr^{-1} which was similar to the rates recorded in recent sediments of Chile's Northern Patagonia fjords (0.14–0.70 cm yr^{-1}; Salamanca and Jara, 2003; Sepúlveda et al., 2005).

C_{org} values of surface sediments of the Gulf of Ancud (MD07-3109H) were higher (3.2%) than those recorded by Silva et al. (2009) in recent sediments of the Inner Sea of Chiloé ($C_{org} = 1 \pm 0.6\%$) and were somewhat higher than those observed in the nearby Puyuhuapi Fjord (44°S) ($C_{org} \sim 2\%$, Sepúlveda et al., 2005) where the marine contribution was diluted by increased continental input (Bertrand et al., 2007). Our C/N values fall within the range (6–10) of those reported by Silva and Astorga (2010) for surface sediments in the area of the Gulf of Ancud, where the highest ratios corresponded to areas near the mouths of rivers and were associated with increased terrigenous organic matter inputs.

In accordance with the average stable isotope data ($\delta^{13}C_{org}$: –20.75‰ $\pm$ 0.82, $\delta^{15}N$: 8.7‰ $\pm$ 0.35), the C/N molar (8.76 ± 0.36) and the mixing model used by estimated the contribution of organic matter sources in our core, the organic matter was characterized as largely of marine origin (Meyers, 1997). We suggest that the increased concentrations of both C_{org} and N_{tot} from the 1980s to the present may be due to early diagenesis in the top $\sim$10 cm of the sediment. Other sediment characteristics such as Si_{OPAL} values (6%) and diatom abundances (mean $= 4 \times 10^7$ valves g^{-1}) in the Gulf of Ancud were found similar to those for other Patagonian fjords ($6.4 \pm 3.7\%$ Inner Sea of Chiloé, Silva et al., 2009; 4–5%, 1×10^7 valves g^{-1} in Puyuhuapi, and 6–10%, 3×10^7 valves g^{-1} Jacaf fjord, Rebolledo et al., 2005, 2008).

Although limited by the different sedimentary and environmental settings, we attempted to compare our results for the Gulf of Ancud with other fjord systems worldwide. In the northern Patagonia fjords, C_{org} values were higher than those reported for the east Greenland fjords ($< 1\%$; Smith et al., 2002). The values fell within the range of those reported for the deep central basin of Saanich Inlet, Canada (1–5%; Gucluer and Gross, 1964), and were somewhat lower than the contents given for Effingham Inlet, Canada (5%; Dallimore et al., 2005) and Koljö Fjord, Sweden (6%; McQuoid and Nordberg, 2003). Diatom abundances in surface sediments of the Gulf of Ancud were very similar to those found Effingham Inlet, Canada (10^7–10^8 valves g^{-1}; Hay et al., 2003) and Saanich Inlet, Canada (McQuoid and Hobson, 1997). Our C/N values were somewhat lower than in Nordåsvannet Fjord, Norway (10.5–12.7; Müller, 2001) and much lower than in Sagenay Fjord, Canada (19.6–25.6; Louchouarn et al., 1997), whereas our $\delta^{13}C_{org}$ and C/N values were similar to those found in Lynn Canal, SW Alaska ($\delta^{13}C = -20.4$ and C/N = 9.6; Walinsky et al., 2009).

5.2. Changes in rainfall and Puelo river streamflow in the twentieth century and their association with ENSO events

From the climatic time-series records it was evident the dramatic decline in rainfall and Puelo River streamflow since the late 1970s and early 1980s. This pattern may be related to the important thinning of the glaciers in Northern Patagonia from the second half of the twentieth century (Masiokas et al., 2008), apparently associated with a greater recurrence of El Niño events after the 1980s along with an important decrease in Northern Patagonia rainfall (Aravena and Luckman, 2008) and Puelo River streamflow (Urrutia et al., 2005; Lara et al., 2008; León-Muñoz et al., this issue). In our record, we also observed a greater abundance of freshwater diatoms at the base of the core, followed by fluctuating values for the period 1940–1980 AD and lower abundances since the late 1980s. This observation coincided with the decreasing trend in freshwater diatoms registered previously in the Puyuhuapi Channel (Rebolledo et al., 2005). The diminished precipitation and, in turn, the lower Puelo River streamflow may have contributed to the declining input of nutrients such as silicic acid derived from the continent available for the growth of diatoms in the photic layer. Our sediment record showed this notorious decline in both the concentrations and accumulations of Si_{OPAL} and siliceous microfossils, accompanied by an important increment of *Rhizosolenia pungens* over the past 20 years. We hypothesize that the increased abundance of *Rhizsolenia pungens* may be due to the decrease in silicate associated with the lower rainfall and river streamflows. This species is weakly silicified and, therefore, it is adapted to lower silicate and higher nutrient (N) contents (Alves-de-Souza et al., 2008). This diatom species is mainly found in brackish waters (Hasle and Syvertsen,

1996) and has been recorded in high concentrations in the water column associated with coastal fronts and fjord areas (Sancetta et al., 1991). It is also important to note that *Rhizosolenia pungens* first occurs in our sediment record of the Gulf of Ancud in ~1900 AD (Fig. 5), coinciding with its occurrence in the Puyuhuapi fjord (44°S; Rebolledo et al., 2005). There is no record of *R. pungens* in sediments older than 1900 AD in the above mentioned settings or in the Jacaf fjord (44°S; Rebolledo et al., 2008). The first occurrence of this species in Northern Patagonia fjords can be linked to transport and introduction into the area by ships' ballast water. The construction of the port of Puerto Montt began around 1888 AD, allowing a greater exchange with ports in Europe (Data from Harbor of Puerto Montt, 2010). The appearance of *Rhizosolenia pungens* in the sedimentary record has been reported for other fjords in the Northern Hemisphere such as Saanich Inlet, British Columbia, around 1940 AD, and was also associated with the ballast water of ships (e.g., McQuoid and Hobson, 1997; Hay et al., 2007).

6. Conclusions

The paleoclimate reconstruction for the recent sediments of the Gulf of Ancud (core MD07-3109H) offers evidence of changing productivity, diatom assemblages, and contributions of freshwater associated with local (fluctuations in rainfall and Puelo River streamflow) and global (El Niño) events. Our record of productivity based on the mass accumulation rates of organic carbon, total nitrogen, Si_{OPAL}, and total diatoms showed a clear decreasing pattern from 1960 AD to the present. This marked reduction in productivity was associated with decreased precipitation and Puelo River streamflow (41°S), as well as a warmer and more stratified water column, especially since the 1980s. The sediments from the Gulf of Ancud are characterized by organic matter that is marine in origin, as reflected by geochemical ($\delta^{13}C_{org}$, C/N molar) and biological (siliceous microfossils) proxies. The appearance of *Rhizosolenia pungens* in sediments younger than ~1900 AD can be used as a stratigraphic marker in the future for paleoclimate reconstructions in the zone. This study provides the basis for future paleoclimatic reconstructions in the area. It is important to conduct experiments with nutrients, salinity, and temperature to estimate the behavior and ecology of key species such as *R. pungens* that cause harmful algal blooms in southern Chile.

Acknowledgements

This project was funded by FONDECYT post-doctorate project #3085045 (L. Rebolledo) and partially by FONDECYT project #1080187 (J.L. Iriarte) and the Center for Oceanographic Research in the eastern South Pacific (COPAS) of the Universidad de Concepción (project #150100007). We thank Dr. Sandor Mulsow, Instituto de Geociencias, Universidad Austral de Chile, for the use of the HAPS sampler and Dr. Gabriel Vargas and Christian Nievas, Facultad de Ciencias Físicas y Matemáticas, Departamento de Geología, Universidad de Chile, for their help with the use of the Mastersizer 2000. We also thank Dr. Catherine Kissel, chief scientist of the PACHIDERME cruise and the crew of the R/V *Marion Dufresne* for a very successful cruise.

References

Ahumada, R., Rudolph, A., 2004. Trace metals and other constitutive components in two sediments cores from a remote glacier-fed estuarine lagoon in Southern Chile. Estuar. Coast. Shelf Sci. 59, 231–236.

Alves-de-Souza, C., González, M., Iriarte, J.L., 2008. Functional groups in marine phytoplankton assemblage dominated by diatoms in fjords of southern Chile. J. Plankton Res. 30 (11), 1233–1243.

Appleby, P.G., Oldfield, F., 1978. The calculation of lead-210 dates assuming a constant rate supply of unsupported ^{210}Pb to the sediment. Catena 5, 1–8.

Araneda, A., Torrejón, F., Aguayo, M., Torres, L., Cruces, F., Cisternas, M., Urrutia, R., 2007. Historical records of San Rafael glacier advances (North Patagonian Icefield): another clue for 'Little Ice Age' timing in Chile? The Holocene 17 (7) 989–1000.

Aravena, J.C., Luckman, B.H., 2008. Spatio-temporal rainfall patterns in southern South America. Int. J. Climatol.). doi:10.1002/JOC.1761.

Avaria, S., Cassis, D., Muñoz, P., Vera, P., 1997. Distribución del microplancton marino en aguas interiores del sur de Chile en octubre de 1995. Comité Oceanográfico Nacional 20, 107–123.

Bertrand, S., Hughen, K., Sepúlveda, J., Pantoja, S., Lange, C., 2007. Late Holocene climate variability of Northern Patagonia reconstructed by a multi-proxy analysis fjord sediments (44–47°S). European Geosciences Union (EGU), Vienna, Austria. Geophysical Research Abstracts 9, 01568.

Bevington, P., Robinson, K., 1992. Error analisis. In: Bevington, P., Robinson, K. (Eds.), Data Reduction and Error Análisis for the Physical Sciences. WCB/McGraw-Hill, New York, USA, pp. 38–52.

Bloesch, J., Evans, R.D., 1982. Lead-210 dating of sediments compared with accumulation rates estimated by natural markers and measured with sediment traps. Hydrobiologia 92, 579–587.

Borgel, R., 1970. Geomorfología de las regiones australes de Chile. Rev. Geol. Chile 21, 135–140.

Brower, J.E., Zar, J.H., Von Ende, C.N., 1998. Field and Laboratory Methods for General Ecology. McGraw-Hill, Dubuque, Iowa, USA 194 pp.

Buschmann, A.H., Cabello, F., Young, K., Carvajal, J., Varela, D.A., 2009. Salmon aquaculture and coastal ecosystem health in Chile: analysis of regulations, environmental impacts and bioremediation systems. Ocean Coast. Manage. 52, 243–249.

Cáceres, M., Valle-Levinson, A., Atkinson, L., 2003. Observations of cross-channel structure of flow in an energetic tidal channel. J. Geophys. Res. 108 (c4) 11–1:11–10.

CALIB 5.0.2, 2009. Calib radiocarbon calibration, data available on the Word Wide Web, accessed 6 August 2009 at URL 〈http://calib.qub.ac.UK/calib/calib.html〉.

CENDHOC, 2009. Centro Nacional de Datos Hidrográficos y Oceanográficos de Chile, data available on the Word Wide Web, accessed 20 May 2009 at URL 〈http://www.shoa.cl/cendhoc/cimar–10/index.html〉.

Cochran, J.K., Frignani, M., Salamanca, M., Belluci, L.G., Guerzoni, S., 1998. Lead-210 as a tracer of atmospheric input of heavy metals in the northern Venice Lagoon. Mar. Chem. 62, 15–29.

Cupp, E.E., 1943. Marine plankton diatoms of the west coast of North America. Bulletin of the Scripps Institution of Oceanography 5, 1–238.

Dallimore, A., Thomson, R.E., Bertram, M.A., 2005. Modern to Late Holocene deposition in an anoxic fjord on the west coast of Canada: implications for regional oceanography, climate and paleoseismic history. Mar. Geol. 219, 47–59.

Dávila, P., Figueroa, D., Müller, E., 2002. Freshwater input into the coastal ocean and its relation with the salinity distribution off austral Chile (35°–55°S). Cont. Shelf Res. 22, 521–534.

DGA, 2005. Dirección General de Aguas, data available on the Word Wide Web, accessed 10 December 2005 at URL 〈http://www.dga.cl.html〉.

Flynn, W.W., 1968. The determination of low levels of Polonium 210 in environmental materials. Anal. Chem. Acta 43, 221–227.

González, H.G., Calderón, M.J., Castro, L., Clement, A., Cuevas, L., Daneri, G., Iriarte, J.L., Lizárraga, L., Martínez, R., Menschel, E., Silva, N., Carrasco, C., Valenzuela, C., Vargas, C.A., Molinet, C., 2010. Primary production and its fate in the pelagic food web of the Reloncaví Fjord and plankton dynamics of the Interior Sea of Chiloé, Northern Patagonia, Chile. Mar. Ecol. Prog. Ser. 402, 13–30.

Gucluer, S.M., Gross, M.G., 1964. Recent marine sediments in Saanich inlet, a stagnant marine basin. Limnol. Oceanogr. 9, 359–376.

Harbor of Puerto Montt, 2010. Puerto de Puerto Montt, data available on the Word Wide Web, accessed 15 February 2010 at URL 〈http://www.empormontt.cl/historia_2.html〉.

Hasle, G.R., Syvertsen, E.E., 1996. Marine diatoms. In: Tomas, C.R. (Ed.), Identifying Marine diatoms and Dinoflagellates. Academic Press, Inc., San Diego, pp. 5–385.

Hay, M.B., Pienitz, R., Thomson, R.E., 2003. Distribution of diatom surface sediment assemblages within Effingham Inlet, a temperate fjord on the west coast of Vancouver Island (Canada). Mar. Micropaleontol. 48, 291–320.

Hay, M.B., Dallimore, A., Thomson, R.E., Calvert, S.E., Pienitz, R., 2007. Siliceous microfossil record of late Holocene oceanography and climate along the west coast of Vancouver Island, Brithish Columbia (Canada). Quat. Res. 67, 33–49.

Hughen, K.A., Baillie, M.G.L., Bard, E., Beck, J.W., Bertrand, C.J.H., Blackwell, P.G., Buck, C.E., Burr, G.S., Cutler, K.B., Damon, P.E., Edwards, R.L., Fairbanks, R.G., Friedrich, M., Guilderson, T.P., Kromer, B., McCormac, G., Manning, S., Ramsey, C.B., Reimer, P.J., Reimer, R.W., Remmele, S., Southon, J.R., Stuiver, M., Talamo, S., Taylor, F.W., van der Plicht, J., Weyhenmeyer, C.E., 2004. Marine04 marine radiocarbon age calibration, 0–26 cal kyr BP. Radiocarbon 46, 1059–1086.

Iriarte, J.L., González, H.E., Liu, K.K., Rivas, C., Valenzuela, C., 2007. Spatial and temporal variability of chlorophyll and primary productivity in surface waters of southern Chile (41.5–43°S). Estuar. Coast. Shelf Sci. 74, 471–480.

KNMI, 2009. Royal Netherland Meteorological Institute, data available on the Word Wide Web, accessed 23 August 2009 at URL 〈http://climexp.knmi.nl/getstations.cgi.html〉.

Lara, A., Villalba, R., Urrutia, R., 2008. A 400-year tree-ring record of the Puelo River summer-fall streamflow in the Valdivian Rainforest eco-region. Climate Change 86, 331–356.

León-Muñoz, J., Soto, D., Lara, A., Iriarte, J. Influence of the streamflow regime of an Andean river on temporal variability of salinity and dissolved oxygen in a North Patagonian fjord, Chile (41. 6°S). Cont. Shelf Res., this issue.

Louchouarn, P., Lucotte, M., Canuel, R., Gagné, J.P., Richard, L.P., 1997. Sources and early diagenesis of lignin and bulk organic matter in the sediments of the Lower St. Lawrence Estuary and the Saguenay Fjord. Mar. Chem. 58, 3–26.

Masiokas, M.H., Villalba, R., Luckman, B.H., Lascano, M.E., Delgado, S., Stepanek, P., 2008. 20th-century glacier recession and regional hydroclimatic changes in northwestern Patagonia. Global Planet. Change 60, 85–100.

McCaffrey, R., Thomson, J.A., 1980. Record of the accumulation of sediment and trace metals in the Conneticut salt marsh. Adv. Geophys. 22, 165–236.

McQuoid, M.R., Hobson, L.A., 1997. A 91–year record of seasonal and interannual variability of diatoms from laminated sediments in Saanich Inlet, British Columbia. J. Plankton Res. 19, 173–194.

McQuoid, M.R., Nordberg, K., 2003. Environmental influence on the diatom and silicoflagellate assemblages in Koljö fjord (Sweden) over the last two centuries. Estuaries 26, 927–937.

Meyers, P.A., 1997. Organic geochemical proxies of paleoceanographic paleolimnologic and paleoclimatic processes. Org. Geochem. 27, 213–250.

Miller, A., 1976. The climate of Chile. In: Schwerdtfeger, W. (Ed.), World Survey of Climatology, vol. 12. Elsevier, Amsterdam, pp. 113–145.

Mortlock, R., Froelich, P., 1989. A simple method for the rapid determination of biogenic opal in pelagic marine sediments. Deep-Sea Res. 36, 1415–1426.

Mulsow, S., Piovano, E., Cordoba, F., 2009. Recent aquatic ecosystem response to environmental events revealed from ^{210}Pb sediment profiles. Mar. Pollut. Bull. 59, 175–181.

Müller, A., 2001. Geochemical expressions of anoxic conditions in Nordåsvannet, a land-locked fjord in Western Norway. Appl. Geochem. 16, 363–374.

NOAA, 2005. Nacional Oceanic and Atmospheric Administration, data available on the World Wide Web, accessed 10 September 2005 at URL 〈http://www.ncdc.noaa.gov/oa/climate/research/sst/sst.php〉.

NOAA, 2009. Nacional Oceanic and Atmospheric Administration, data available on the Word Wide Web, accessed 24 August 2009 at URL 〈http://www.cdc.noaa.gov/people/klaus.wolter/MEI.html〉.

OceanTest equipment, 2010. Ocean Test equipment, data available on the Word Wide Web, accessed 24 February 2010 at URL 〈http://www.oceantestequip.com/seafloorsamp.html〉.

Otero, L., 2006. La huella del fuego, Pehuen Editores Historia de los bosques nativos y cambios en el paisaje del sur de Chile, Santiago, Chile 160 pp.

Pinto, L., Bonert, C., 2005. Origen y distribución espacial de hidrocarburos alifáticos en sedimentos de Seno Aysén y Canal Moraleda, Chile Austral. Ciencia y Tecnología del Mar. 28 (1), 35–44.

Rebolledo, L., Lange, C.B., Figueroa, D., Pantoja, S., Muñoz, P., Castro, R., 2005. 20th century fluctuations in the abundance of siliceous microorganisms preserved in the sediments of the Puyuhuapi Channel (44°S), Chile. Rev. Chil. Hist. Nat. 78 (3), 469–488.

Rebolledo, L., Sepúlveda, J., Lange, C., Pantoja, S., Bertrand, S., Hughen, K., Figueroa, D., 2008. Late Holocene marine productivity changes in Northern Patagonia–Chile inferred from a multi-proxy analysis of Jacaf channel sediments. Estuar. Coast. Shelf Sci. 80, 314–322.

Rivera, P., 1981. Beiträge zur Taxonomie und Verbreitung der Gattung Thalassiosira Cleve. Bibliotheca Pycologica 56, 1–220.

Rojas, N., Silva, N., 2005. Early diagenesis and vertical distribution of organic carbon and total nitrogen in recent sediments of the Chilean fjords: boca del Guafo (43°47′ S) to canal Pulluche (45° 49′ S). Investigaciones Marinas 33 (2), 183–194.

Round, E.E., Crawford, R.M., Mann, D.G. (Eds.), 1990. The Diatoms: biology and Morphology of the Genera. Cambridge University Press, Cambridge.

Salamanca, M.A., Jara, B., 2003. Distribución y acumulación de plomo (Pb y ^{210}Pb) en sedimentos de los fiordos de la XI región, Chile. Ciencia y Tecnología del Mar. 26, 61–71.

Sancetta, C., Villareal, T., Falkowski, P., 1991. Massive fluxes of Rhizosolenid diatoms: a common occurrence? Limnol. Oceanogr. 36 (7), 1452–1457.

Schrader, H., Gersonde, S., 1978. Diatoms and silicoflagellates in the eight meters section of the lower Pliocene on Campo Rosello. Utrecht Micropaleontological Bulletin 17, 129–176.

Sepúlveda, J., Pantoja, S., Hughen, K., Lange, C., González, F., Muñoz, P., Rebolledo, L., Castro, R., Contreras, S., Ávila, A., Rossel, P., Lorca, G., Salamanca, M., Silva, N., 2005. Fluctuations in export productivity over the last century from sediments of a southern Chilean fjord (44°S). Estuar. Coast. Shelf Sci. 65, 587–600.

Sepúlveda, J., Pantoja, S., Hughen, K.A., Bertrand, S., Figueroa, D., León, T., Drenzek, N.J., Lange, C.B., 2009. Late Holocene sea-surface temperature and precipitation variability in northern Patagonia, Chile (Jacaf Fjord, 44°S). Quaternary Research 72 (3), 400–409.

Sepúlveda, J., Pantoja, S., Hughen, K.A. Sources and distribution of organic matter in northern Patagonian fjords, Chile (∼44–47°S): a multi-tracer approach for carbon cycling assessment. Cont. Shelf Res., this issue.

Silva, N., Prego, R., 2002. Carbon and nitrogen spatial segregation and stoichiometry in the surface sediments of southern Chilean inlets (41–56°S). Estuar. Coast. Shelf Sci. 55, 763–775.

Silva, N., Sievers, H., Prado, R., 1995. Características oceanográficas y una proposición de circulación, para algunos canales australes de Chile entre 41° 20′ y 46°40′ S. Revista Biología Marina 30 (2), 207–254.

Silva, N., Calvete, C., Sievers, H., 1997. Características oceanográficas físicas y químicas de canales australes chilenos entre Puerto Montt y laguna San Rafael (Crucero CIMAR Fiordo 1). Ciencia y Tecnología del Mar. 20, 23–106.

Silva, N., Haro, J., Prego, R., 2009. Metals background and enrichment in the Chiloé Interior Sea sediments (Chile). Is there any segregation between fjords, channels and sounds? Estuar. Coast. Shelf Sci. 82 469–476.

Silva, N., Astorga, M.I., 2010. Textura, materia orgánica y composición química elemental (C y N) de sedimentos marinos superficiales de la zona Puerto Montt a Boca del Guafo (Norpatagonia chilena). Lat. Am. J. Aquat. Res. 38 (1), 1–14.

Silva, N., Vargas, C.A., Prego, R., Land-ocean distribution of allocthonous organic matter in the surface sediments of the Chiloé and Aysén interior seas (Chilean Northern Patagonia). Cont. Shelf Res., this issue.

Sims, P.A. (Ed.), 1996. An Atlas of British Diatoms. Biopress Ltd, Bristol United Kingdom.

Smith, L.M., Alexander, C., Jennings, A.E., 2002. Accumulation in East Greenlad fjords and on the continental shelves and adjacent to the Denmark Strait over the last century based on ^{210}Pb geochronology. Arctic 55, 109–122.

Tello, A.G., Rodríguez-Benito, C., 2009. Characterization of mesoscale spatio-temporal patterns and variability of remotely sensed Chla and SST in the Interior sea of Chiloé (41.4–43.5°S). Int. J. Remote Sens. 30 (6), 1521–1536.

Thornton, S.F., McManus, J., 1994. Application of organic carbon and nitrogen stable isotope and C/N ratios as source indicators of organic matter provenance in estuarine systems: evidence from the Tay Estuary. Scotland. Estuar. Coast. Shelf. Sci. 38, 219–233.

Turekian, K., Cochran, K., Benninger, L., Aller, R., 1980. The sources and sinks of nuclides in Long Island Sound. Adv. Geophys. 22, 129–163.

Urrutia, R., Lara, A., Villalba, R., 2005. ¿Cómo ha variado la disponibilidad de agua en la ecorregión de los bosques valdivianos en los últimos siglos? Revista Ambiente y Desarrollo 21 (3) 48–57.

Walinsky, S.E., Prahl, F.G., Mix, A.C., Finney, B.P., Jaeger, J.M., Rosen, G.P., 2009. Distribution and composition of organic matter in surface sediments of coastal Southeast Alaska. Cont. Shelf Res. 29, 1565–1579.

Warren, C., Aniya, M., 1999. The calving glaciers of southern South America. Global Planet. Change 22, 59–77.

Witkowski, A., Lange-Bertalot, H., Metzeltin, D., 2000. Diatom flora of marine coast I. Iconographia diatomologica annotated diatom micrographs. Diversity Taxonomy–Identification. Koeltzs Scientific Books, Königstein, Germany, 925.